A&A 417, 973–979 (2004)
DOI: 10.1051/0004-6361:20040011

Astronomy & Astrophysics

Observation of the Monoceros Loop *SNR* region with the HEGRA system of IACTs

F. A. Aharonian[2], A. G. Akhperjanian[7], M. Beilicke[4], K. Bernlöhr[2], H.-G. Börst[5], H. Bojahr[6], O. Bolz[2], T. Coarasa[3], J. L. Contreras[1], J. Cortina[10], S. Denninghoff[3], M.V. Fonseca[1], M. Girma[2], N. Götting[4], G. Heinzelmann[4], G. Hermann[2], A. Heusler[2], W. Hofmann[2], D. Horns[2], I. Jung[2], R. Kankanyan[2], M. Kestel[3], A. Kohnle[2], A. Konopelko[2], H. Kornmeyer[3], D. Kranich[3], H. Lampeitl[4], M. Lopez[1], E. Lorenz[3], F. Lucarelli[1], O. Mang[5], H. Meyer[6], R. Mirzoyan[3], A. Moralejo[1], E. Ona-Wilhelmi[1], M. Panter[2], A. Plyasheshnikov[2,8], G. Pühlhofer[2], R. de los Reyes[1], W. Rhode[6], J. Ripken[4], G. Rowell[2], V. Sahakian[7], M. Samorski[5], M. Schilling[5], M. Siems[5], D. Sobzynska[2,9], W. Stamm[5], M. Tluczykont[4], V. Vitale[3], H. J. Völk[2], C. A. Wiedner[2], and W. Wittek[3]

[1] Universidad Complutense, Facultad de Ciencias Físicas, Ciudad Universitaria, 28040 Madrid, Spain
[2] Max-Planck-Institut für Kernphysik, Postfach 103980, 9029 Heidelberg, Germany
[3] Max-Planck-Institut für Physik, Föhringer Ring 6, 80805 München, Germany
[4] Universität Hamburg, Institut für Experimentalphysik, Luruper Chaussee 149, 22761 Hamburg, Germany
[5] Universität Kiel, Institut für Experimentelle und Angewandte Physik, Leibnizstraße 15-19, 24118 Kiel, Germany
[6] Universität Wuppertal, Fachbereich Physik, Gaußstr. 20, 42097 Wuppertal, Germany
[7] Yerevan Physics Institute, Alikhanian Br. 2, 375036 Yerevan, Armenia
[8] On leave from Altai State University, Dimitrov Street 66, 656099 Barnaul, Russia
[9] Home institute: University Lodz, Poland
[10] Institut de Física d'Altes Energies, UAB, Edifici Cn, 08193, Bellaterra (Barcelona), Spain

Received 13 June 2003 / Accepted 9 December 2003

Abstract. The array of 5 imaging atmospheric Čerenkov telescopes (IACTs) deployed at La Palma (Canary Islands), and operated by the HEGRA (High Energy Gamma Ray Astronomy) collaboration, was used for observations of the Monoceros Loop *SNR* region for a total of about 120 hrs and 20 hrs in ON-source and OFF-source mode, respectively. The giant molecular cloud Rosette Nebula appears in the sky region, close to the south-east part of the *SNR* rim. Using the HEGRA system of IACTs of rather large field of view (4.3 degree in diameter), we have mapped the extended sky region of $3^\circ \times 3^\circ$ associated with the Monoceros *SNR*/Rosette Nebula, which is centered towards the hard spectrum X-ray point source SAX J0635+533. The EGRET unidentified source of diffuse γ-ray emission (3EG J0634+0521) observed in the energy range between 100 MeV–10 GeV, was effectively in the field of view of our present observations. Also, the GeV source GeV J0633+0645 was within the available field of view. The performance of the IACTs array reveals an energy threshold of 500 GeV and an angular resolution of 0.1° for γ-rays. In what follows, we present the result of the data analysis and its physical interpretation.

Key words. gamma rays: observations – ISM: supernova remnants – ISM: individual objects: Monoceros Loop *SNR*

1. Introduction

The origin of cosmic-rays (CRs) with energies $E \leqslant 10^{15}$ eV, the so-called *galactic cosmic-rays*, is a long-standing problem which still has not found a definitive solution. Supernova remnants (*SNR*s) are widely believed to be the sites of galactic CR acceleration (e.g. see Drury 1991). We still do not have clear experimental evidence that the nuclear component of CRs is accelerated there, even though theory predicts that they should be very efficiently accelerated (Berezhko & Völk 2000; Ellison et al. 2000). If the *SNR*s are the actual sites of CR production, interactions between the accelerated particles and the local interstellar matter have to occur. Originally, Drury et al. (1994) calculated the expected γ-ray fluxes from *SNR*s assuming the model of diffusive shock acceleration and π°-production of secondary γ-rays by charged CRs interacting with the local swept-up interstellar matter. An evident clue of CR acceleration in *SNR*s would be the detection by current satellite and ground-based detectors of high-energy γ-rays from *SNR*s which expand into or near dense matter regions, like giant molecular clouds (Aharonian et al. 1994). The EGRET instrument on board the Compton Gamma-Ray Observatory has found MeV–GeV γ-ray signals associated with at least three such *SNR*s: IC443 and γ-Cygni (Esposito et al. 1996) and the Monoceros *SNR*/Rosette Nebula region (Jaffe et al. 1997; Romero et al. 1999). It is believed that the observed γ-ray

Send offprint requests to: F. Lucarelli, e-mail: lucarel@gae.ucm.es

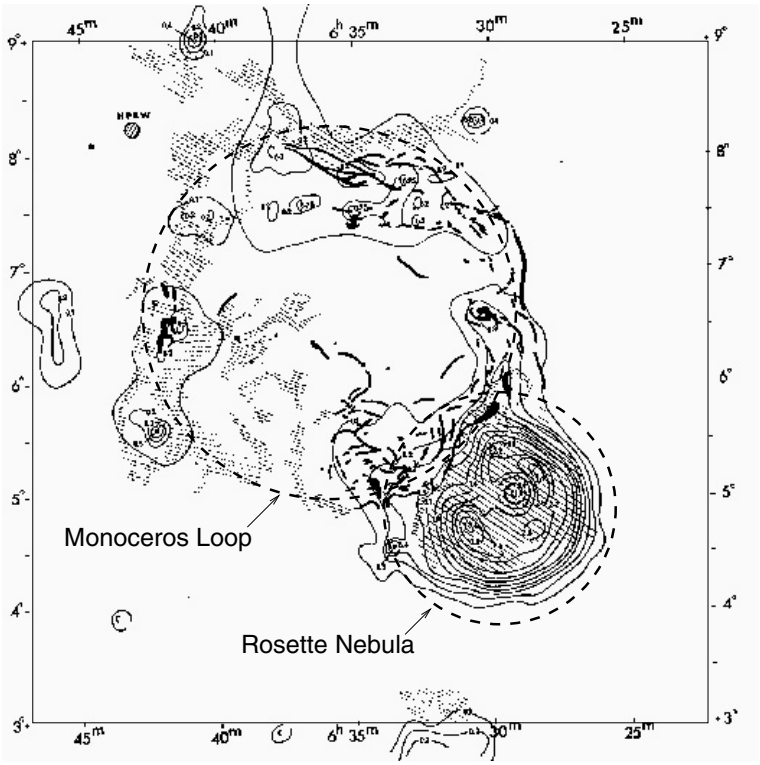

Fig. 1. Radio and optical map of the Monoceros region taken from Davis et al. (1978). Contour levels show the radio observation at 2650 MHz. Thick lines represent the optical bright filaments while shaded regions show the faint optical nebulosity. The Rosette Nebula is visible in the south-east portion and dominates the radio map. Coordinates are referred to the 1950 epoch.

emission is the result of the interaction of protons, accelerated by *SNR* shock waves, with the supernova matter itself or with the swept-up matter of the adjacent molecular clouds. Detection of these *SNR*s at TeV energies using ground-based imaging Čerenkov telescopes will offer almost direct evidence of CR acceleration at *SNR* shocks.

Despite the theoretical expectations, only three *SNR*s have been detected as TeV γ-ray emitters by ground-based Čerenkov telescopes: RX J1713.7-3946 (Enomoto et al. 2002) and SN1006 (Tanimori et al. 1998) by the CANGAROO Čerenkov telescope and CASSIOPEIA A (Aharonian et al. 2001a) by the HEGRA IACTs system. Very recently, SN1006 was confirmed by the stand-alone HEGRA CT1 telescope (Vitale 2003). For SN1006 and CAS A, the TeV emission has been explained by the inverse-compton scattering of non-thermal relativistic electrons on the cosmic microwave background photons. The measured TeV energy spectrum of RX J1713.7-3946 matches that expected in the case of hadronic origin of the emission, yet there is much debate about that (Butt et al. 2002).

After rather short exposures of about 10 hrs, upper limits for IC 443, γ-Cygni and Monoceros Loop *SNR* have been reported by the Whipple Collaboration (Buckley et al. 1998; Lessard et al. 1999). Further upper limits on the γ-ray flux above 1 TeV for IC 443 and Tycho were derived from data taken with the HEGRA IACT array for, respectively, 30 hrs and 60 hrs of observation (Heß et al. 1997; Aharonian et al. 2001b).

2. The Monoceros Loop and its surroundings

The Monoceros Loop (*SNR* G205.5+0.5) was recognized as *SNR* by Davies (1963) from 237 MHz radio observations. At optical wavelengths, the Monoceros Loop appears as an irregular bright ring of emission about 3.5° in diameter, centered on RA = $6^{\rm h}38^{\rm m}43^{\rm s}$, Dec = +6°30.2′ (J2000) (see Fig. 1). The optical and radio properties of the Monoceros *SNR*/Rosette Nebula have been studied in great detail by Davies et al. (1978) and Graham et al. (1982), respectively. The distance to the Monoceros Loop derived by Graham et al. (1982) is about 1.6 kpc. The corresponding radial extension is about 50–60 pc, which places it in the vicinity of the Rosette Nebula (estimated distance: 1.39 ± 0.1 kpc (Hensberge et al. 2000)). The estimated age of the *SNR* is $3-15 \times 10^4$ yr, where the shock expands in the Sedov phase. According to Davies et al. (1978), the filamentary structures visible in the optical band for the southern part of the remnant are a proof of the possible interaction between the loop and the molecular cloud (see Fig. 1). Despite the fact that no detection of maser emission has been reported in the radio survey at 1720.5 MHz by Frail et al. (1996), an interaction between the two objects is not excluded.

Observation of the $J = 1-0$ rotational transition of carbon monoxide (CO) at 115 GHz, makes it possible to trace the presence of molecular clouds interacting with expanding *SNR* shells. The CO emission intensity map of the Monoceros Loop region has shown enhanced density coinciding with the Rosette Nebula (Torres et al. 2003).

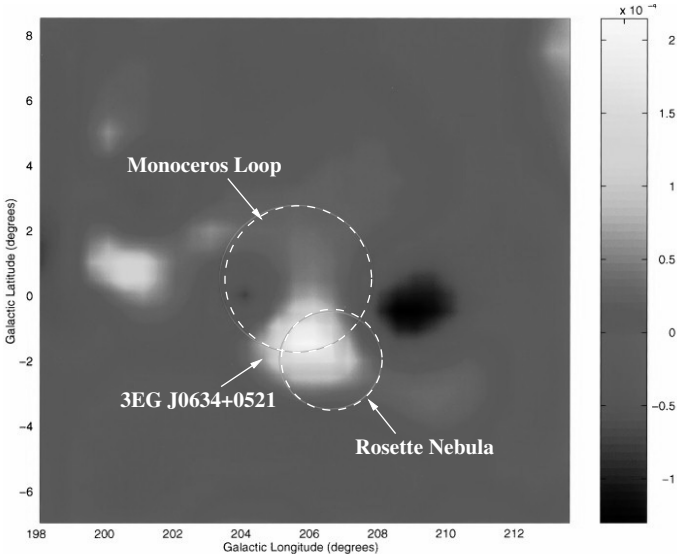

Fig. 2. EGRET detection plot from Jaffe et al. (1997). Shown are the approximate extension and position of the Monoceros Loop (big circle) and of the Rosette Nebula (small circle).

The approximate nucleon density of the Rosette Nebula is 40 cm^{-3} as reported by Williams et al. (1995). However, there is a large uncertainty in the nucleonic density which is averaged over the highly inhomogeneous cloud. Such a cloud might have clumps with enhanced density up to $n_{\rm H} \leqslant 500$ cm^{-3}, as in the case of IC 443 (Dickman et al. 1992).

As the Monoceros Loop is still in its Sedov phase of expansion, X-ray fluxes from this region can be expected. Leahy et al. (1985, 1986) mapped the Monoceros Loop using the EINSTEIN X-ray satellite and detected regions of diffuse X-ray emission. These regions are located on the rim of the remnant and they coincide with the densest region of optical filaments which show a high hardness ratio (>0.3)[1]. Leahy et al. (1986) found that the Monoceros *SNR* emitted a 0.5–3 keV X-ray flux of 1.5×10^{-10} erg cm^{-2} s^{-1}. An observation carried out with the BeppoSAX satellite (Kaaret et al. 1999) discovered a hard spectrum X-ray point source (SAX J0635+0533) within the 95% probability circle of the EGRET detection, which was later identified as a binary pulsar (Cusumano et al. 2000). The unabsorbed flux from the source is 1.2×10^{-11} ergs cm^{-2} s^{-1} in the 2–10 keV band. No extended emission has been reported from the BeppoSAX observations. However, the field of view of the BeppoSAX observation was relatively small compared with the EINSTEIN scan and the angular extension of the Monoceros *SNR*.

EGRET detected from the region associated with the Monoceros *SNR*/Rosette Nebula (see Fig. 2) an extended γ-ray emission in the energy range from 100 MeV up to 10 GeV at a 7σ confidence level (Jaffe et al. 1997). This emission was interpreted as γ-rays from the decay of π^0's produced by the interaction of shock accelerated protons with the ambient matter. The γ-ray flux for $E \geqslant 100$ MeV is $(5.36 \pm 0.43) \times 10^{-7}$ photons cm^{-2} s^{-1}. This source is listed in the 3rd EGRET catalog with the name 3EG J0634+0521 (Hartman et al. 1999). Another unidentified EGRET source, named 3EG J0631+0642, is present in the same region, lying on the eastern part of the *SNR* rim. This source emits photons with energy above 1 GeV and is listed in the catalog of GeV sources as GeV J0633+0645 (Lamb & Macomb 1997).

[1] Hardness ratio = $(H-S)/(H+S)$ with H = 0.8 to 3.5 keV counts, S = 0.2 to 0.8 keV counts.

Table 1. Summary of the data taken towards the direction of the Monoceros/Rosette region with the HEGRA system of IACTs. $T_{\rm OBS}$ is the total observational time. $T_{\rm EFF}$ is the effective observational time after data cleaning. $R_{\rm CR}$ is the cosmic-ray detection rate and $\langle ZA \rangle$ is the average zenith angle of the observation.

Obs. mode	$T_{\rm OBS}$ [hrs]	$T_{\rm EFF}$ [hrs]	$R_{\rm CR}$ [Hz]	$\langle ZA \rangle$ [deg]
ON-source	119	114	≃14	26.7
OFF-source	19	19	≃14	26.7

3. HEGRA data analysis

The Monoceros *SNR*/Rosette Nebula region was observed mostly in ON-source mode accompanied by approximately 20 hrs of OFF-source runs taken at ±5° away from the source in right ascension. For the ON-source observations, the BeppoSAX source SAX J0635+0533 (RA = $6^{\rm h}35^{\rm m}17.4^{\rm s}$, DEC = +5°33′21″ (J2000)) was adjusted to the center of the joint field of view (FoV) of the telescopes. Table 1 summarizes the observation times and the average CR detection rates and zenith angles (ZA) of the observations. An accurate data selection, based on the rejection of all runs with actual rates less than 30% off the expected rates calculated according to the ZA, was performed and a total amount of about 5 hr was rejected.

A number of checks was applied to the cleaned data in order to test their quality, e.g. verification of the constancy of the CR rejection factor over the observation period and the homogeneity in the camera response over the FoV, control of stability in the *mscw*-distribution of CR events on a run-by-run basis etc. All the controls have shown the good quality of the data used.

A preliminary analysis of a first data sample of about 40 hrs (Lucarelli et al. 2001a) already reported a positive excess at the level of 2.5σ within the 3EG J0634+0521 error circle, while a second preliminary analysis of the whole data sample based on the technique discussed in Konopelko et al. (2002), reported a positive excess at the level above 3σ (Lucarelli et al. 2001b). In what follows we have used a more sophisticated analysis to determine the position of the reconstructed events and a new background estimation.

The stereoscopic reconstruction of air showers with the HEGRA system of IACTs allows us to calculate the right ascension (RA) and declination (Dec) for each individual event as well as the angular slopes of the shower axis in the joint focal plane. Table 2 summarizes the criteria used for the selection of *good stereo events* in search for TeV γ-ray emission within the quite large EGRET 3EG J0634+0521 and 3EG J0631+0642 error circles ($\theta_{95\%} = 0.67°$ and $\theta_{95\%} = 0.46°$, respectively) and, serendipitously, over a large fraction of the entire FoV of the HEGRA telescope system. Details about the telescope system

Table 2. Requirements for selection of good quality γ-like events.

Number of operating telescopes:	≥4
Zenith angle range:	<45°
Algorithm of stereo reconstruction:	#3
Number of triggered telescopes:	≥3
Minimum image num. of photo-electrons:	40
Image center of gravity:	≤1.7°
Reconstructed core position:	<500 m.
Mean scaled WIDTH cut:	*mscw* < 1.1

and the analysis technique can be found in Aharonian et al. (1999) and Konopelko et al. (1999).

For the reconstruction of the shower arrival direction, three basic algorithms are available (Hofmann et al. 1999). We have used the one described as #3 in Hofmann et al. (1999), which takes into account the errors in the determination of the center of gravity and orientation of the Čerenkov images, providing a better determination (hence, better angular resolution) of the reconstructed source position. The other two algorithms give comparable results. Furthermore, we have used in the analysis only events with at least three triggered telescopes, which provide good angular resolution and efficient γ/hadron separation.

In the event selection, we have selected only Čerenkov images with a total charge great than 40 photo-electrons (ph.e.) and with their center of gravity within 1.7° from the camera center, in order to reject images which are truncated by the camera edge. We have also accepted only showers with a reconstructed core position within 500 m. from the central telescope.

The image shape cut used in the rejection of the CR background events is the so-called *mean scaled width (mscw)* cut (Konopelko et al. 1999). The image parameter *mscw* is calculated by averaging the *scaled width* from each triggered telescope. The images are scaled according to the value expected for γ-ray induced air showers (calculated beforehand through Monte Carlo simulations), which ultimately depends upon the ZA of the observation, the impact parameter and the image parameter *size*. A tight image cut of $mscw < 1.1$ has been applied to the selected data in order to reject a large fraction (up to 70%) of the hadron induced events.

The average zenith angle of the Monoceros observations was around 26° (see Table 1). The corresponding energy threshold (defined as the peak of the differential γ-ray detection rate) for the Monoceros data sample is of about 800 GeV.

4. Significance of excess from the interaction region Monoceros *SNR*/Rosette Nebula

Based on physical arguments and numerical computations as well as on the presence of the extended EGRET emission, we formulate the hypothesis that the TeV γ-rays emission may occur within the interaction region between the *SNR* shock front and the molecular cloud. This region appears to be inside the 3EG J0634+0521 error circle. The γ-ray emission is expected to follow the radio profile of the shell (Berezhko et al. 2002) and can be substantially enhanced by the interaction with the dense Rosette Nebula molecular cloud (Aharonian et al. 1994).

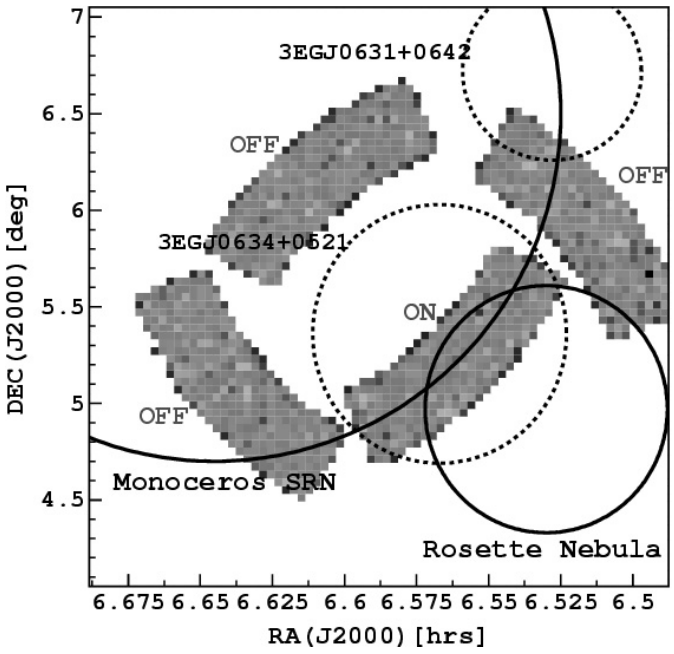

Fig. 3. Scheme of the search for TeV γ-ray emission from the interaction region between the Monoceros Loop *SNR* shock front and the Rosette Nebula (ON region). The three OFF regions are used for the estimation of the cosmic-ray background contamination. The radial fall-off in the camera response has been corrected in order to have a uniform FoV. Shown are also the approximate extents of the Monoceros Loop and Rosette Nebula (solid line circles) and the 95% error circles of the EGRET sources 3EG J0634+0521 and 3EG J0631+0642 (dashed line circles).

Thus, we decided to estimate the significance of the excess coming from this region, counting as ON all events with reconstructed arrival directions within a circular sector placed just where the *SNR* shell and the molecular cloud supposedly collide (see Fig. 3). Taking into account the uncertainties in the position and extension of the Monoceros Loop *SNR* shell as well as the angular dimension of the Rosette Nebula, we have assumed as angular size of the interaction region 0.4° in the radial direction. In order to estimate the CR background contamination (OFF) for this region and derive the corresponding significance, we have accumulated OFF events from three sky regions of the same shape and size chosen from different parts of the FoV (see Fig. 3). Due to the limited statistics of the runs taken in OFF-source mode, we have estimated the CR background content directly from the large sample of ON-source data. A correction for the fall-off of the camera response along the radial direction (Pühlhofer et al. 2003) has been applied in order to have a FoV as uniform as possible: this makes it possible to place the regions for the background estimation (the OFF regions in Fig. 3) at different distances from the center of the camera with respect to the ON region. The OFF regions have been selected in areas where we do not a priori expect TeV γ-ray emission, nor have found it previously. The selection cuts summarized in Table 2 have been applied to the data.

In general, the calculation of the excess significance for a source must take into account the difference in exposure time between the ON-source and OFF-source runs, defined through

Table 3. Analysis results for the interaction region Monoceros Loop *SNR*-Rosette Nebula. Upper limits at 99% CL are also reported, both in [ph cm^{-2} s^{-1}] and Crab Flux units. The energy threshold is 800 GeV.

Background	*ON*	*OFF*	α	*Excess*	$S\ [\sigma]$	$\Phi_{\gamma,\mathrm{UL}}$ [10^{-12} cm^{-2}s^{-1}]	$\frac{\Phi_{\gamma,\mathrm{UL}}}{\Phi_{\mathrm{Crab}}}$
3 OFF reg.	7585	21 666	0.333	363	+3.6	2.2	0.09

the $\alpha = T_{\mathrm{ON}}/T_{\mathrm{OFF}}$ scaling factor. In our case, since we only make use of ON-source data, $T_{\mathrm{ON}} = T_{\mathrm{OFF}}$. However, we have used 3 sky regions of the same shape and size as the ON region to estimate the background contamination. Thus, a factor $\alpha = 1/3$ has to be included in the estimation of the excess significance.

The number of ON and OFF counts, the correspondent scaling factor α, the number of excess events and the corresponding significance calculated according to Eq. (17) in Li & Ma (1983), are given in Table 3.

Table 3 reports also the 99% Coincidence Level (CL) upper limit for the selected extended region, calculated using the procedure described in Helene (1983). The upper limit is given in Crab units as well as in units of [10^{-12} ph cm^{-2}s^{-1}].

5. Serendipitous search for γ-ray sources

Besides the search for γ-ray extended emission from the interaction region, we have performed a serendipitous search for point-like and extended γ-ray emission all over the available FoV and, in particular, within the very large EGRET sources error circles. We have divided the FoV into angular bins of size much smaller than the angular resolution of the instrument, accumulating ON events for each point of the grid within a search window with radius comparable to the angular resolution of the instrument. This procedure is equivalent to a *smoothing* of the sky map of the reconstructed event directions, and makes it possible to look for statistical correlation between adjacent bins. The CR background content (OFF) for each grid point was estimated directly from the big sample of ON-source data. Figure 4 shows a $3^\circ \times 3^\circ$ sky map seen at $0.04^\circ \times 0.04^\circ$. For each bin, the number of excess events was calculated using the so called *ring background model* for the background estimation, after the application of the standard image shape cut *mscw* < 1.1: at each bin, the excess is estimated within a radius of $\theta = 0.13^\circ$ and the corresponding OFF is taken from an annular ring ($r_1 = 0.25^\circ$, $r_2 = 0.35^\circ$) centered at the same bin position and in the same *mscw* regime. The size of the search window is comparable to the angular resolution of the HEGRA system of IACTs, which was calculated from a sample of Crab data taken at the same periods and at the same zenith angles (using the same cuts as reported in Table 2). The corresponding distribution of the excess significance per bin is centered at zero with rms $\simeq 1\sigma$, proving the suitability of the applied method. Interestingly, after the serendipitous search, a pair of hot spots appeared within the EGRET error circle of the 3EG J0634+0521 source (that is, the interaction region) (see Fig. 4), showing an overall significance between 3 and 4σ. However, a serendipitous search for point-like sources like this one is subject to statistical penalties or *trial factors*, due to the fact that the hypothesis (no source of γ-rays in any of the bins) has to be tested over a large number of bins and, eventually, the estimated post-trial significance of these features is fully in agreement with a background fluctuation.

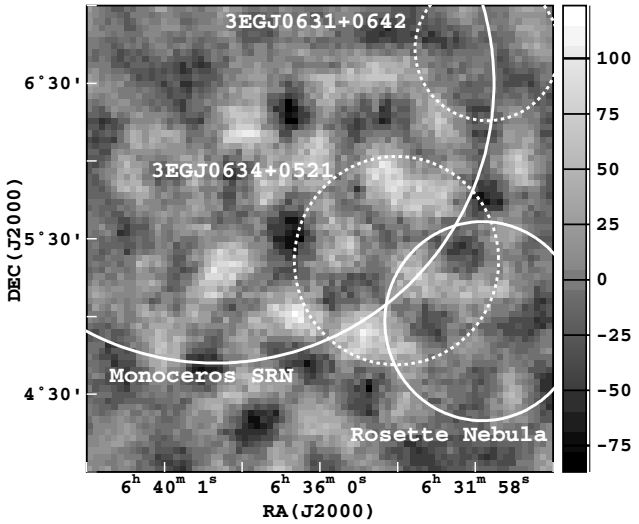

Fig. 4. $3^\circ \times 3^\circ$ smoothed sky map of the TeV excess events coming from the direction of the Monoceros Loop *SNR* (bin size: $0.04^\circ \times 0.04^\circ$). At each bin the excess is estimated using the ring background model described in the text with a point-like source search window of $\theta = 0.13^\circ$. Superimposed are the approximate extents of the Monoceros Loop and Rosette Nebula and the 95% error circles of the EGRET sources 3EG J0634+0521 and 3EG J0631+0642.

6. Upper limits on 3EG J0631+0642

As we have mentioned previously, there is another unidentified EGRET source in the Monoceros Loop *SNR* region, numbered 3EG J0631+0642 (also listed as GeV source (GeV J0633+0645) in Lamb & Macomb (1997), which is clearly visible on the sky maps shown before. It is centered at 1.47° from the tracking point of the observations of 3EG J0634+0521, and it is within the FoV of the HEGRA system of IACTs. Interestingly, it also lies on the rim of the Monoceros *SNR* shell. We have estimated the upper limit on γ-ray emission from the sky region coinciding with the 3EG J0631+0642 error circle ($\theta_{95\%} = 0.46^\circ$) using two OFF regions of the same size and placed at the same distance from the center of FoV. Table 4 summarizes the significance and the 99% CL upper limit. No hints of γ-ray emission are reported.

Table 4. Analysis results for 3EG J0631+0642 (GeV J0633+0645). Upper limits at 99% CL. The energy threshold is 800 GeV.

Background	*ON*	*OFF*	α	*Excess*	$S\,[\sigma]$	$\Phi_{\gamma,\mathrm{UL}}$ [10^{-12} cm^{-2}s^{-1}]	$\frac{\Phi_{\gamma,\mathrm{UL}}}{\Phi_{\mathrm{Crab}}}$
2 OFF reg.	4266	8268	0.5	132	+1.6	1.7	0.07

7. Discussion and conclusions

The Monoceros Loop *SNR* region was observed with the HEGRA stereoscopic system of 5 IACTs for about 120 hrs in 1999/2001.

No significant emission at TeV energies from the assumed interaction region between the expanding shell and the molecular cloud has been found. Thus, we report a 3σ upper limit of 2.2×10^{-12} ph cm^{-2} s^{-1} (0.09 Crab unit) from this region.

A serendipitous search over a large part of the 4.3° FoV subtended by the HEGRA IACTs system has shown the presence of a pair of structures within the error circle of the EGRET unidentified source 3EG J0634+0521, but their post-trial significance is in agreement with that expected for background fluctuations.

Torres et al. (2003) postulate that the extended emission detected by EGRET from 3EG J0634+0521 could be the result of a composite emission: part of the γ-rays would come from the binary pulsar SAX J0635+0533 and the remainder from the interaction region between the expanding shell and the Rosette Nebula. Unfortunately, we could not confirm this scenario.

We can estimate the expected γ-ray rate from the EGRET source 3EG J0634+0521 in case the EGRET spectrum extends up to TeV energies. The reported 3EG J0634+0521 flux is $F_\gamma(> 100\ \mathrm{MeV}) = (2.55 \pm 0.51) \times 10^{-7}$ ph cm^{-2} s^{-1}. Extrapolating this flux to TeV energies one can calculate the corresponding γ-ray rate over the interaction region we have selected, ~1/3 of the 95% EGRET error circle. Considering an effective area of 10^9 cm^2 at 1 TeV (Konopelko et al. 1999), the corresponding γ-ray rate would be $R_\gamma \approx 9 \times 10^{-3}$ Hz.

The average CR rate for the HEGRA system of IACTs is about 17 Hz (Pühlhofer et al. 2003). The corresponding CR rate for a sky region with a point-like source extension ($\theta_0 = 0.13°$) will be thus given by: $R_{\mathrm{CR}}^{\mathrm{pt}} = 17 \cdot (\theta_0/R_{\mathrm{cam}})^2 \approx 6 \times 10^{-2}$ Hz where $R_{\mathrm{cam}} \simeq 2.3°$ is the half opening angle of the PMT camera.

The expected signal-to-noise ratio for an extended source of extension θ_{ext} is given by (Konopelko et al. 2002):

$$S/N = R_\gamma \kappa_\gamma / \left[R_{\mathrm{CR}}^{\mathrm{pt}} \kappa_{\mathrm{CR}} \cdot (\theta_{\mathrm{ext}}/\theta_0)^2 \right]^{1/2} \; T_{\mathrm{OBS}}^{1/2}$$

where $(\theta_{\mathrm{ext}}/\theta_0)^2$ is the ratio between the extended and the point-like source areas (around 10 in our case); κ_γ and κ_{cr} are the γ-rays and CR acceptances (that is, the fraction of remaining events after applying the image shape cut on *mscw*), respectively, and T_{OBS} is the duration of the observation. For $T_{\mathrm{OBS}} \approx 114$ hrs and a cut at $mscw < 1.1$ (to which correspond the acceptances $\kappa_\gamma = 0.68$ and $\kappa_{\mathrm{CR}} = 0.04$, for a minimum number of telescopes triggered by a single event of 3 out of 5 (Konopelko et al. 2002)) we would end up with $S/N \approx 25$, a value which is clearly in contradiction with our observations and with the upper limit previously reported by the WHIPPLE group (Lessard et al. 1999). Therefore, a noticeable steepening in the EGRET spectrum towards TeV energies is plausible.

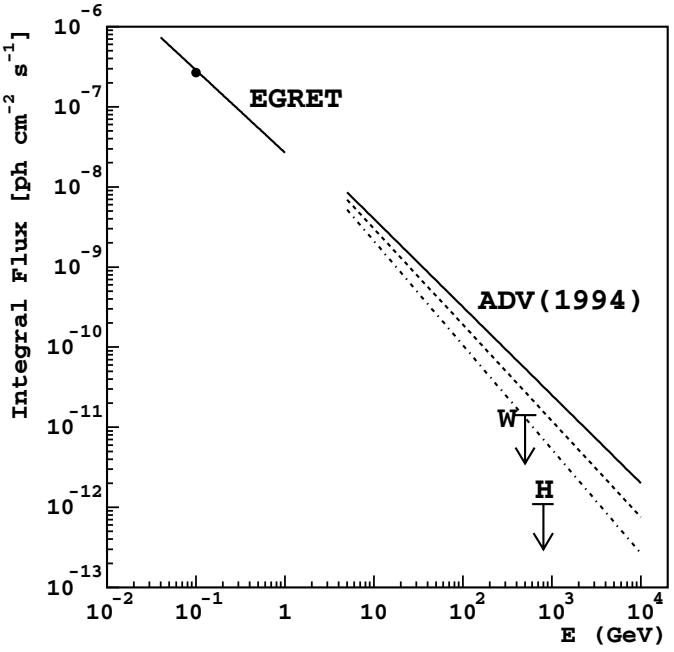

Fig. 5. Upper limits for 3EG J0634+521 (Monoceros Loop/Rosette Nebula interaction region) from the present work (H) and a previous measurement by the Whipple telescope (W) (see text for reference). We also show the measured EGRET integral flux and the expected integral γ-ray fluxes from π°-decay based on the predictions of the ADV model and considering a mean matter density of the target (Rosette Nebula) of $n \simeq 40$ cm^{-3}. The solid, dashed and dash-dotted lines represent the predictions for three different assumptions on the spectral index of the differential energy spectrum of a population of shock-wave-accelerated protons ($\mathrm{d}N/\mathrm{d}E \propto E^{-\alpha+1}$): $\alpha = 2.1$, 2.2 and 2.3, respectively.

We can now compare the derived upper limit with the predictions of the γ-ray flux above 1 TeV based on the Aharonian, Drury & Völk (1994) (ADV) model assuming the EGRET flux reported above with a measured spectral index $\alpha_\gamma = 2.03$ (see Fig. 5).

The expected TeV γ-ray flux from π°-decay produced in the interaction between shock accelerated protons and the ambient matter is given by (Aharonian et al. 1994):

$$F_\gamma(\geq E) = f_\alpha \times 10^{-10} \left(\frac{E}{1\ \mathrm{TeV}} \right)^{-\alpha+1} A\ \mathrm{ph\ cm^{-2}\ s^{-1}}$$

where α is the expected value of the spectral index of the differential energy spectrum of the accelerated protons and

$$A = \theta \left(\frac{E_{\mathrm{SN}}}{10^{51}\ \mathrm{erg}} \right) \left(\frac{d}{1\ \mathrm{kpc}} \right)^{-2} \left(\frac{n}{1\ \mathrm{cm^{-2}}} \right)$$

is a dimensionless factor which takes into account the fraction of the supernova (SN) explosion energy converted into CR energy density, the distance to the SN, and the density of the medium. In our case, $d \simeq 1.6$ kpc (Graham et al. 1982), $n \simeq 40$ cm^{-3} and $\theta = 0.1$.

Figure 5 shows the expected integral fluxes for three different assumptions on the accelerated proton spectral index, together with the HEGRA and WHIPPLE upper limits. The WHIPPLE upper limit is based on an exposure of about 13 hrs and is also at 99% CL and valid for the extended emission from the interaction region (Lessard et al. 1999). Because of the longer observation time, our upper limit is lower than the WHIPPLE upper limit by almost an order of magnitude.

Our upper limit is clearly below the simple predictions of TeV emission from π°-decay based on the ADV model. Thus, the interaction region has so far not been proven to be a site of multi-TeV particle acceleration. Nevertheless, the presence of some structures within the EGRET error circle makes this region worthy of further study with future Čerenkov telescopes.

Concerning 3EG J0631+0642, the error circle of the GeV source is still located on the rim of the expanding shell and, specifically, in a region where bright optical filaments are visible (see Fig. 1). Thus, gas compressed with high density is also present in this part of the rim. We might expect a similar proton acceleration mechanism by shock waves and enhanced γ-ray emission by π^0 decay due to the higher-density matter. In this case, the non-detection at TeV energies also implies some absorption at the source, or a different emission mechanism of the GeV photons detected.

Acknowledgements. The support of the HEGRA experiment by the German Ministry for Research and Technology BMBF and by the Spanish Research Council CICYT (FPA2000-1802-C02-01) is acknowledged. We are grateful to the Instituto de Astrofísica de Canarias for the use of the site and for providing excellent working conditions.

References

Aharonian, F. A., Drury, L. O'C., & Völk, H. J. 1994, A&A, 285, 645
Aharonian, F. A., Akhperjanian, A. G., Barrio, J. A., et al. (HEGRA collaboration) 1999, A&A, 349, 11
Aharonian, F. A., Akhperjanian, A. G., Barrio, J. A., et al. (HEGRA collaboration) 2001a, A&A, 370, 112
Aharonian, F. A., Akhperjanian, A. G., Barrio, J. A., et al. (HEGRA collaboration) 2001b, A&A, 373, 292
Berezhko, E. G., & Völk, H. J. 2000, Astropart. Phys., 14, 201
Berezhko, E. G., Ksenofontov, L. T., & Völk, H. J. 2002, A&A, 395, 943
Buckley, J. H., Akerlof, C. W., Carter-Lewis, D. A., et al. 1998, A&A, 329, 639
Butt, Y. M., Torres, D. F., Romero, G. E., et al. 2002, Nature, 418, 499
Cusumano, G., Maccarona, M. C., Nicastro, L., et al. 2000, ApJ, 528, L25
Davies, R. D. 1963, Observatory, 83, 172
Davies, R. D., Elliott, K. H., Goudis, C., et al. 1978, A&AS, 31, 271
Dickman, R. L., Snell, R. L., Ziurys, L. M., et al. 1992, ApJ, 400, 203
Drury, L. O'C. 1991, in Astrophysical aspects of the most energetic cosmic-rays (Singapore: World Scientific), 252
Drury, L. O'C., Aharonian, F. A., & Völk, H. J. 1994, A&A, 287, 959
Ellison, D. C., Berezhko, E. G., & Baring, M. G. 2000, ApJ, 540, 292
Enomoto, R., Tanimori, T., Naito, T., et al. (CANGAROO collaboration) 2002, Nature, 416, 823
Esposito, J. A., Hunter, S. D., Kanbach, G., et al. 1996, ApJ, 461, 820
Frail, D. A., Goss, W. M., Reynoso, E. M., et al. 1996, AJ, 111, 1651
Graham, D. A., Haslam, C. G. T., Salter, C. J., et al. 1982, A&A, 109, 145
Hartman, R. C., Bertsch, D. L., Bloom, S. D., et al. 1999, ApJS, 123, 79
Helene, O. 1983, Nucl. Instr. & Methods, 212, 319
Hensberge, H., Pavloski, K., & Verschueren, W. 2000, A&A, 258, 553
Heß, M., et al. (HEGRA collaboration) 1997, in Proc. of the 25th ICRC, Durban, 3, 229
Hofmann, W., Jung, I., Konopelko, A., et al. 1999, Astropart. Phys., 12, 135
Jaffe, T., Bhatta charya, D., Dixon, D. D., et al. 1997, ApJ, 484, L129
Kaaret, P., Piraino, S., Halpera, J., et al. 1999, ApJ, 523, 197
Konopelko, A., Lucarelli, F., Lampeitl, H., & Hofmann, W. 2002, J. Phys. G: Nuclear and Particle Phys., 28, 2755
Konopelko, A., Hemberger, M., Aharonian, F. A., et al. 1999, Astropart. Phys., 10, 275
Lamb, R. C., & Macomb, D. J. 1997, ApJ, 488, 872
Leahy, D. A., Naranan, S., & Singh, K. P. 1985, MNRAS, 213, 15
Leahy, D. A., Naranan, S., & Singh, K. P. 1986, MNRAS, 220, 501
Lessard, R. W., et al. 1999, in Proc. of the 26th ICRC, Salt Lake City, 3, 488
Li, T., & Ma, Y. 1983, ApJ, 273, 317
Lucarelli, F., Konopelko, A., Rowell, G., & Fonseca, V. 2001a, in Proc. of the Int. Symp. on High Energy Gamma-Ray Astronomy (Heidelberg), ed. AIP Proc. Ser. (NY), 779
Lucarelli, F., Konopelko, A., & Fonseca, V. 2001b, in Proc. of the 27th ICRC, Hamburg, 6, 2461
Pühlhofer, G., Bolz, O., Götting, N., et al. (HEGRA collaboration) 2003, Astropart. Phys., 20, 267
Romero, G. E., Benaglia, P., & Torres, D. F. 1999, A&A, 348, 868
Tanimori, T., Hayami, Y., Kamei, S., et al. 1998, ApJ, 497, L25
Torres, D. F., et al. 2003, to be appeared in Phys. Rep. [astro-ph/0209565]
Vitale, V., et al. (HEGRA), in Proc. of the 28th ICRC, Tsukuba, 2, 2389
Williams, J. P., Blitz., L., & Start, A. 1995, ApJ, 451, 252